scientific reports

Check for updates

OPEN

Genetically engineered BMSCs promote dopamine secretion and ameliorate motor dysfunction in a Parkinson's disease rat model

Chunjing Wang[1,2,4], Yang Liu[1,2,4], Junyan Chang[1,2], Yiqin He[1,2], Pan Yang[1,2], Jingjing Fu[1,2], Wanying Du[1,2], Caiyun Ma[1,2], Gaofeng Liu[1,2], Yu Guo[1,3]✉ & Changqing Liu[1,2]✉

Regenerative therapy based on mesenchymal stem cells (MSCs) is regarded as a promising strategy for treating Parkinson's disease (PD). Previous studies have shown that mesenchymal stem cell transplantation has the potential to treat Parkinson's disease, but its specific mechanism of action is still unclear. In the present study, we generate genetically engineered bone marrow mesenchymal stem cells (BMSCs) encoding three critical genes (TH, DDC, and GCH1) for dopamine synthesis (DA-BMSCs). The DA-BMSCs maintain their MSCs characteristics and stable ability to secrete dopamine after passage. Moreover, the DA-BMSCs survived and functioned in a rat model of PD treated with 6-OHDA 8 weeks after transplantation. Histological studies showed that DA-BMSCs could differentiate into various functional neurons and astrocytes, and DA-BMSCs derived mature dopaminergic neurons extended dense neurites into the host striatum. Importantly, DA-BMSCs promoted the reconstruction of midbrain dopamine pathways by upregulating striatal dopamine and 5-HT levels and downregulating the levels of inflammatory factors including IL-6, TNF-α, and IL-10. These findings suggest that engineered mesenchymal stem cell transplantation for dopamine synthesis may be an attractive donor material for treating Parkinson's disease.

Keywords Bone marrow mesenchymal stem cells, Dopamine, Dopamine decarboxylase, GTP cyclohydrolase 1, Tyrosine hydroxylase, Parkinson's disease

Abbreviations

PD	Parkinson's disease
MSCs	Mesenchymal stem cells
TH	Tyrosine hydroxylase
DDC	Dopamine decarboxylase
GCH1	GTP cyclase 1
DA	Dopamine
BMSCs	Bone mesenchymal stem cells
DA-BMSCs	The BMSCs cell line stably overexpressing DA
MFB	Medial forebrain bundle
SN	Substantia nigra
BH4	Tetrahydrobiopterin
GDNF	Glial cell derived neurotrophic factor
SHH	Sonic hedgehog
BDNF	Brain-derived neurotrophic factor
CDNF	Cerebral dopamine neurotrophic factor
H&E	Hematoxylin and eosin
TH-DAB	TH-3,3′-Diaminobenzidine tetrahydrochloride
SYN	Synaptophysin
TNF-α	Tumor necrosis factor-alpha

[1]Anhui Engineering Research Center for Neural Regeneration Technology and Medical New Materials, Bengbu Medical University, Bengbu 233000, China. [2]School of Life Sciences, Bengbu Medical University, Bengbu 233000, Anhui, China. [3]School of Laboratory Medicine, Bengbu Medical University, Bengbu 233000, Anhui, China. [4]Chunjing Wang and Yang Liu contributed equally to this work. ✉email: guoyu@bbmu.edu.cn; lcq7813@bbmu.edu.cn

CINC-1	Cytokine-induced neutrophil chemoattractant
CNS	Central nervous system
5-HT	Serotonin
IACUC	Institutional Animal Care and Use Committee
BSD	Blasticidin
6-OHDA	6-Hydroxydopamine
APO	Apomorphine
FGF2	Fibroblast growth factor 2
NEAA	Non-essential amino acid
BSA	Bovine serum albumin

Parkinson's disease (PD) is the second most common neurodegenerative disorder after Alzheimer's disease, characterized by the progressive loss of dopaminergic neurons in the substantia nigra (SN)[1]. In addition to the predominant motor symptoms such as bradykinesia, resting tremor, rigidity, and postural instability, a wide range of non-motor symptoms like cognitive impairments, depression, other emotional changes, and sleep difficulties are highly prevalent in PD patients[2,3]. Motor symptoms in PD are effectively treated using dopamine precursor levodopa (L-DOPA), dopamine agonists, monoamine oxidase and catechol-O-methyl-transferase inhibitors to restore dopamine levels[4]. As the disease progresses, these medications diminish the therapeutic effect and result in a range of serious side effects, such as dyskinesia, hallucinations, and psychiatric problems[5,6]. Because the main hallmark of PD is the progressive loss of DA neurons in the substantia nigra (SN), cell transplantation has been considered as an effective therapeutic alternative to DA neuron loss[7–9].

Dopamine biosynthesis is regulated by three key rate-limiting enzymes in midbrain dopaminergic neurons, tyrosine hydroxylase (TH), GTP cyclohydrolase 1 (GCH1), and DOPA decarboxylase (DDC)[10]. Tyrosine hydroxylase (TH) is present predominantly in dopaminergic neurons in the substantia nigra pars compacta (SNpc) and catalyzes the synthesis of L-DOPA from tyrosine in the presence of tetrahydrobiopterin (BH4), as an essential cofactor synthesized by GTP cyclase 1 (GCH1)[11,12]. L-DOPA is converted to dopamine by DOPA decarboxylase (DDC). Previous studies have shown that increasing dopamine levels in the striatum is the most effective treatment for Parkinson's disease (PD)[13]. One of the current strategies for the treatment of PD is to increase the level of dopamine by overexpressing these rate-limiting enzyme genes[14]. Recently, the lentivirus and adenovirus vectors carrying some genes related to the PD pathways, such as glial cell derived neurotrophic factor (GDNF) and sonic hedgehog (SHH), can effectively improve the motor behaviors or physiological functions of PD animals[15,16]. Moreover, the overexpression of TH, DDC, and GCH1 genes significantly promoted DOPA synthesis and improved neurological deficits in PD animal models[17,18]. However, direct delivery of the three genes into the striatum by viral infection still faces many obstacles. For example, it is difficult to finely evaluate and control which cells or how many cells in the striatum could be successfully infected by delivered viruses. In addition, lentiviruses and AAV viruses as delivery tools will cause safety issues in gene therapy. Importantly, these limitations may be resolved by developing genetically engineered cells to allow for continuous and stable synthesis of dopamine, and cell transplantation can be carried out after evaluating the safety and characteristics of these cells.

Mesenchymal stem cells (MSCs) are a diverse subset of multipotent precursors present in the stromal fraction of many adult tissues, such as bone marrow, adipose tissue, umbilical cord, lung tissue, and placenta[19,20]. Due to low immunogenicity and immunomodulatory abilities, MSCs have been used as the most promising cell sources for the treatment of many diseases, including autoimmune disease, regenerative medicine, and inflammation-associated disease[21,22]. Previous studies revealed that transplantation of MSCs can significantly improve movement disorders and protect dopaminergic neurons from apoptosis, which is considered a promising treatment for PD[23]. Human MSCs can also inhibit the synthesis of α-synuclein and have neuroprotective effects on neurons in a Parkinsonian model[24]. Moreover, the genetically modified MSCs can overexpress neurotrophic factors such as brain-derived neurotrophic factor (BDNF), Glial-cell-derived neurotrophic factor (GDNF), and cerebral dopamine neurotrophic factor (CDNF), increase the number of dopaminergic neurons in substantia nigra, and improve motor functional recovery by preserving the nigrostriatal pathway in PD animal models[25,26].

In this study, the three genes TH, DDC, and GCH1 were introduced into rat bone marrow mesenchymal stem cells (BMSCs) to obtain the genetically modified BMSCs with the stable ability to synthesize dopamine (DA-BMSCs). And, the genetically modified DA-BMSCs were stereotactically transplanted into the right medial forebrain bundle (MFB) of 6-hydroxydopamine (6-OHDA)-lesioned parkinsonian rats to detect their functional effects in vivo. Our results showed that DA-BMSC grafts can effectively improve motor deficits and cognitive impairment in PD rats in the long term by restoring extracellular concentrations of dopamine, which may be an attractive donor material for transplantation therapy for PD patients.

Materials and methods

Animals

All Sprague-Dawley (SD) rats were provided by the Animal Experimental Center of Shandong Province (license No. SCXK [Lu] 2019-0003). The use of animals and all experimental procedures were approved by the Institutional Animal Care and Use Committee (IACUC) for Ethics of Bengbu Medical College (Bengbu, China; approval no. 2022-139). All sections of this report adhere to the ARRIVE Guidelines 2.0 for reporting animal research[27], and all procedures were performed in accordance with the guidelines and regulations.

Construction and packaging of lentiviral vectors

The full-length Human CDS sequences of TH (NM_199292), DDC (NM_001082971), and GCH1 (NM_001024024) were cloned into two lentivirus plasmids, respectively (Hanbio Biotechnology, Co., Ltd. Shanghai, China). The

cDNA of the TH gene was inserted downstream of the CMV promoter and upstream of fluorescent protein gene EF1-mCherry and resistance cassette puromycin (Puro) to construct Lenti-CMV-TH-EF1-mCherry-T2A-Puro^R plasmid. The cDNAs of DDC and GCH1 genes were inserted downstream of the CMV promoter and upstream of fluorescent protein gene EF1-ZsGreen and resistance cassette Blasticidin S (BSD) to construct Lenti-CMV-DDC-T2A-GCH1-EF1-ZsGreen-P2A-BSD^R plasmid. The plasmids vector maps are provided in Supplementary Fig. 1 (Fig. S1). The packaged lentiviruses were named LV-TH and LV-DDC-GCH1 respectively.

Isolation and identification of bone mesenchymal stem cells

Bone marrow cells were collected from the bone cavity of 4-week-old Sprague-Dawley rats and filtered through a nylon mesh (200 mesh). Bone marrow cells were resuspended at 2×10^5 cells/mL in DMEM/F12 medium supplemented with 10% (v/v) fetal bovine serum(FBS; Gibco, Thermo Fisher Scientific, Waltham, MA, USA), 1mM L-glutaMAX(Gibco), 1% non-essential amino acid (NEAA, Gibco), 10 ng/mL fibroblast growth factor 2 (FGF2; R&D, USA), and 100 U/mL penicillin-streptomycin (Gibco) at 37 °C with 5% CO_2 in a humidified incubator. When reaching about 80–90% confluence, the BMSCs were passaged with 0.25% trypsin/0.01% EDTA or stored in liquid nitrogen for later use (Gibco). Karyotype assessment via chromosomal G-band analysis was performed according to standard protocol[28]. Colony-forming units (CFU) of BMSCs were stained with crystal violet for 30 min and then counted and photographed under a microscope. Colony-forming units were defined as colonies with ≥ 50 cells.

Immunofluorescence staining and flow cytometry analysis

BMSCs cultured on coverslips were fixed with 4% paraformaldehyde for 20 min, followed by permeabilization with 0.2% Triton X-100 for 10 min, and blocked with 5% normal donkey serum (Sigma-Aldrich; Merck KgaA, Darmstadt, Germany) and 3% bovine serum albumin(BSA, Sigma-Aldrich) for 1 h at room temperature. Then, cells were incubated with the following primary antibodies overnight at 4 °C: CD29, CD44, CD73, CD90, CD34, CD45, GABA, DRD1 (1:200; Bioss, Beijing, China), PSD95, OCT4, SOX2, GFAP (1:200; Abcam, Cambridge, MA, USA), TH, SYN (1:500; Abcam), DDC and GCH1 (1:500; Santa Cruz Biotechnology, Santa Cruz, CA, USA), IBA1 (1:500; CST), C3 (1:500; Santa Cruz, CA, USA). After being washed with PBS, the cells were incubated with appropriate secondary antibodies conjugated to either Alexa Fluor 488 (1:500, Invitrogen, Carlsbad, CA, USA), or Cyanine 3 (Cy3) dye (Jackson Immunoresearch, West Grove, PA, USA) for 1 h at room temperature. Then, the cell nuclei were counterstained with DAPI (Beyotime, Shanghai, China) for 10 min. The immunofluorescence results were observed under a multiphoton laser scanning microscope (Olympus, FV1200MPE SHARE, Tokyo, Japan). Expression of BMSCs surface markers (CD29, CD44, CD73, and CD90) and hematopoietic lineage molecular markers (CD34 and CD45) was further detected using a flow cytometer (dxP Athena 1 L-3 L; cytek Biosciences, California, USA) using FlowJo cE V10.1 software (FlowJo LLC) following the previously described method[29]. The catalog numbers for all antibodies used in this research are provided in Table S2.

Western blotting analysis and RT-qPCR

The BMSCs were lysed with RIPA Lysis Buffer containing a protease inhibitor cocktail (Fisher Scientific, USA). Each sample was separated by SDS-PAGE gel electrophoresis with equal amounts of protein (40 μg), electroblotted onto PVDF membranes (0.45 μM; Millipore Sigma), and immunoblotted overnight at 4 °C with the following primary antibodies: anti-TH (1:1 000, Abcam), anti-DDC (1:1 000), anti-GCH1 (1:1 000, Santa Cruz) and anti-GAPDH (1:2 000, Affinity Biosciences, USA). Immunoreactive proteins were incubated with peroxidase-conjugated secondary antibody (1:5000, Jackson ImmunoResearch). The protein bands were then visualized with Clarity Western ECL Blotting Substrates (Bio-Rad Laboratories, Hercules, CA, USA) and quantified using Quantity One software version 1-D (Bio-Rad Laboratories). The catalog numbers for all antibodies used in this research are provided in Table S2.

Total RNAs were extracted from cells using Trizol® reagent (Invitrogen) and reverse transcribed into cDNA using PrimeScript™ RT Reagent Kit (Takara Biotechnology Co., Ltd., Dalian, China) following the manufacturer's protocols. Quantitative real-time polymerase chain reaction was carried out using TB Green Premix Ex Taq II (Takara Bio) with a QuantStudio™ 6 Flex thermocycler (Applied Biosystems, Carlsbad, CA, USA). The ΔΔCT method was used to analyze the data. The primers were synthesized by Sangon Biotech (Shanghai, China) and presented in Table S1. The thermocycling conditions were as follows: Initial denaturation at 95˚C for 30 s, followed by 40 cycles of denaturation or 10 s at 95 °C and 20 s at 60 °C, and GAPDH was used as the internal control.

Lentiviral infection and generation of DA-BMSCs cell line

The initial BMSCs at passage 4 (P4) were transduced with lentiviruses carrying LV-TH with a multiplicity of infection of 10 (MOI:10), LV-DDC-GCH1 with a multiplicity of infection of 10 (MOI:10), or co-transduced with lentiviruses carrying LV-TH (MOI:8) and LV-DDC-GCH1 (MOI:5), in the presence of polybrene (5–10 μg/mL) for 24 h at 37 °C. The infection efficiencies were detected after 72 h of infection with LV-TH and LV-DDC-GCH1 lentiviruses. At day 2 post-transduction, the BMSCs transduced with LV-TH lentiviruses were screened and maintained for 72 h in the presence of 2 μg/mL puromycin to establish an LV-TH-BMSCs cell line. The BMSCs transduced with the LV-DDC-GCH1 lentiviruses were screened in the presence of 1.5 μg/mL Blasticidin S to establish the LV-DDC-GCH1-BMSCs cell line. The BMSCs co-transduced with lentiviruses LV-TH and LV-DDC-GCH1 were screened in the presence of 1.5 μg/mL Blasticidin S and 2 μg/mL puromycin for two weeks to establish DA-BMSCs cell line.

6-Hydroxydopamine (6-OHDA)-lesioned rat model of PD

Forty-eight adult male rats (8–10 weeks, 180–220 g) were used in this study, of which eight rats were used as negative controls (the healthy group). The remaining 40 rats were deeply anesthetized with 3% Sodium Pentobarbital (2.5 mL/kg, intraperitoneally) and fixed on a brain stereotaxic apparatus (Reward Life Technology Co., Ltd.). The anesthetized rats were unilaterally infused with 8 μL 6-OHDA solution (5 mg/mL, dissolved in 0.2% ascorbate saline; Sigma-Aldrich; Merck KGaA) into the right MFB ($n = 40$) at a rate of 0.5 μL/min at the following two coordinates related to the bregma[28].: Anteroposterior (AP)-4.4, mediolateral (ML)-1.0 mm, dorsoventral (DV)-7.8; and AP-4.0, ML-0.8 mm, DV-8.0, and the needle was maintained for an additional 8 min before retraction[30,31]. After surgery, each rat was administered 30 kU penicillin intramuscularly to prevent infection.

Behavioral detection of the parkinsonian rat models

Rotation test. Two weeks after the 6-OHDA injection, the rats were injected intraperitoneally with 0.5 mg/kg apomorphine (APO; Sigma-Aldrich) to induce rotational behavior contralateral to the lesion side to assess motor dysfunction. A rotational speed of ≥ 210 revolutions/30 min was considered as the criterion for successful modeling of rats with PD[7]. Apomorphine-induced rotations in hemiparkinsonian rats were also evaluated at 2, 4, and 8 weeks after cell transplantation.

Rotarod test. Three rats were detected simultaneously on the three channels of a rotarod apparatus (SANS Biotechnology, Jiangsu, China) to evaluate motor coordination[32]. The test was processed at a uniform speed of 40 rpm for 30 min, and each animal completed three trials. The number of turns and the time staying on the rotarod were automatically recorded. The test was performed at 2, 4, and 8 weeks after cell transplantation.

Open field test. The spontaneous locomotive activity of rats was recorded using the open field test in a dark area (100 × 100 × 40 cm) to evaluate excitability and activity. The rats were placed in the center of the open-field apparatus, and the total moving distance of each trial within 5 min was automatically captured and analyzed by the Ethovision XT 10.1 S system (Noldus, Leesburg, Netherlands). Zone heatmaps were generated by tracing the path of the rats in the open field.

Transplantation of DA-BMSCs into the right MFB of parkinsonian rats

To assess the long-term survival and impact of grafted cells, BMSCs were dissociated into single cells by TrypLE (Gibco) and resuspended in serum-free H-DMEM at a cell suspension of 1.25×10^7 cells/mL and stereotactically transplanted into the right MFB of each parkinsonian model rat using the same two stereotaxic coordinates as those used in the PD model. At each site, 8 μL of cell suspension containing 1.0×10^5 cells were injected using a Hamilton microsyringe (Reno, NV, USA) at a rate of 0.5 μL/min[33,34]. The PD model rats were divided randomly into five groups, each consisting of 8 rats ($n = 8$): vehicle group was injected with 8 μL H-DMEM, BMSCs group was injected with 8 μL BMSCs, LV-TH group was injected with 8 μL LV-TH BMSCs, LV-DDC-GCH1 group was injected with 8 μL LV-DDC-GCH1 BMSCs, and DA-BMSCs group was injected with 8 μL DA-BMSCs.

Histology and immunohistochemistry (IHC)

The rats were deeply anesthetized by intraperitoneal injections of 3% Sodium Pentobarbital (50 mg/kg) and transcardially perfused with 200 mL of saline followed by 200 mL of 4% paraformaldehyde (PFA) at 4 and 8 weeks after cell transplantation. Then the rats were cervically dislocated and the perfused brain was collected. The brains were embedded in paraffin, and sectioned coronally into 30 μm-thick slices. Afterward, some paraffin sections were routinely dewaxed and incubated with anti-tyrosine hydroxylase (TH, 1:300; Abcam) antibody overnight at 4 °C. Subsequently, the sections were incubated with an HRP-conjugated goat anti-rabbit secondary antibody (1:1000; Jackson ImmunoResearch) for 1 h at room temperature. The sections were then stained with 3,3′-diaminobenzidine tetrahydrochloride (DAB; Servicebio, Wuhan, China). Additionally, histopathological examination of 3-μm paraffin-embedded sections was routinely performed using an H&E staining kit (Servicebio) according to the manufacturer's protocol. The results of the survival and number of TH^+ cells for the TH-DAB and HE staining were detected by whole-brain scanning using the Nikon Imaging system (Nikon DS-U3, Tokyo, Japan) and the CaseViewer 2.0 software (3DHISTECH Ltd., Budapest, Hungary).

Meanwhile, the whole perfused brains were embedded using OCT embedding and sectioned coronally into 12 μm-thick slices using a microtone cryostat (Leica, CM1950, Wetzlar, Germany), mounted on gelatin-coated glass slides. The survival, migration, and differentiation of transplanted DA-BMSCs in the host brain were determined by immunofluorescence staining. The cryosections were stained with one of the following primary antibodies overnight at 4 °C: anti-TH (1:300), anti-Synaptophysin (1:300; both from Abcam), anti-GFAP (1:200; Santa Crμz), anti-PSD95 (1:200; CST), and anti-GABA (1:300; Sigma-Aldrich). After secondary antibody incubation conjugated to Alexa Fluor 647 (1:500; Jackson lab) for 1 h at room temperature, the immunofluorescence staining results were observed under a fully motorized inverted fluorescence microscope (Zeiss, Observer Z1, Germany).

Enzyme-linked immunosorbent assay (ELISA) test

The levels of pro-inflammatory cytokines (IL-6 and TNF-α) and anti-inflammatory cytokines (IL-10) in the right striatum of different groups at 8 weeks after cell transplantation were evaluated with ELISA kits (Bioss Biotechnology Co, Ltd., China) following the manufacturers' instructions, respective.

HPLC-FLD analysis of DA and 5-HT

Detections of the levels of DA and 5-HT in the cell culture supernatant, serum, and brain tissues were carried out by HPLC analysis. The brain tissue (cortex, hippocampus, and striatum), which weighs about 50 mg, was independently dissected and put into chilled tubes 8 weeks after cell transplantation. The tissues

were homogenized in 10 volumes of cold buffer containing 0.35 M perchloric acid and 1.5 mM cysteine and centrifuged at 18 000 rpm for 10 min at 4℃. Cell supernatant of each group was collected after 48 h of culture. Moreover, the serum of each group and cell supernatant was homogenized in the same way. The clear supernatant of each sample was filtered using the 0.22 μm Millipore membrane and directly injected into an HPLC System (SHIMADZU, Japan). The mobile phase consisted of water containing 50 mM KH_2PO_4, 0.08 mM EDTA (mobile phase A) and methanol (mobile phase B). For reverse phase HPLC with the analytical column, a C18 HPLC column (SHIMADZU, 5 μm, 150 mm × 4.6 mm, Japan) was used. The analysis time per sample was 10 min, and the injection volume for analysis was 20 μL. The column temperature was set at 40 ℃.

Statistical analysis

All statistical analyses and the generation of graphs were done using the GraphPad Prism 7.0 software (GraphPad, San Diego, CA, USA). All quantitative data are presented as the mean ± SEM of the mean for at least three independent experiments. Multiple comparisons were evaluated by one-way ANOVA, followed by Dunnett's multiple comparison test, and multiple comparisons were evaluated by two-way ANOVA, followed by Sidak's multiple comparison test. A statistically significant difference was considered as $P < 0.05$.

Results

Isolation and identification of rat BMSCs

The time flowchart for the establishment of DA-BMSCs that can stably secrete dopamine neurotransmitters was described in Fig. 1A. Primary BMSCs isolated from rat bone marrow adhered to plates and exhibited spindle-shaped or triangular morphology (Fig. 1B). A homogenous population of typical fibroblast-like cells was obtained after two to three passages. Rat BMSCs have greater colony-forming potentials, and the colony-forming rate of passage 4 was 52 ± 4.7% (Fig. 1B). More than 90% of rat BMSCs could highly express the typical MSCs surface antigen markers and the pluripotency markers at passage 4, including CD29, CD44, CD73, CD90, OCT4, and SOX2, and could not express hematopoietic lineage cell markers CD45 and CD34 (Fig. 1C, D). Moreover, the MSCs markers S100A1 and COL1A1 were also highly expressed, and epithelial cell markers CDH1 and MUC1 were not expressed (Fig. 1E). And the original gels are presented in Supplementary Fig. 2 (Fig S2). Chromosome G-banding analysis demonstrated that the BMSCs maintained genetic stability with the frequency of normal diploid karyotypes (2n = 42, XY) was 96.8% at passage 4 (Fig. 1F).

Establishment of DA-BMSCs that can stably secrete dopamine neurotransmitters

Dopamine biosynthesis is driven by three key enzymes TH, DDC, and GCH1 (Fig. 2A). The cDNAs of human *TH*, *DDC*, and *GCH1* genes were subcloned into two lentiviral vectors to construct Lenti-CMV-TH-EF1-mCherry-T2A-Puro^R and Lenti-CMV-DDC-T2A-GCH1-EF1-ZsGreen-P2A-BSD^R plasmids (Fig. 2B). The results indicated that the infection efficiencies of LV-mCherry, LV-TH, LV-ZsGreen, LV-DDC-GCH1, and LV-TH + LV-DDC-GCH1 were 91.6 ± 2.0%, 66.2 ± 0.8%, 84.5 ± 2.5%, 54.3 ± 3.1%, and 51.0% ± 1.9%, respectively (Fig. 2C, D). After 2 weeks of BSD and Puro antibiotic selection, the expression of DDC and GCH1 proteins in the LV-DDC-GCH1 infected cells was significantly upregulated, and the expression of TH protein in the LV-TH infected cells was significantly upregulated (Fig. 2F). Moreover, the LV-TH + DDC-GCH1 co-infected cells exhibited significant over-expression of TH, DDC, and GCH1 protein (Fig. 2E, F). Then, the expression of *TH*, *DDC*, and *GCH1* at the mRNA level was further confirmed by RT-PCR analysis (Fig. 2G, H). The original blots/gels are presented in Supplementary Fig. 2 (Fig. S2). The relative expression of TH was 512.9 ± 96.4% in the LV-TH group, and 306.9 ± 82.4% in the LV-TH + DDC-GCH1 group. The relative expression of DDC was 855.6 ± 278.1% in the LV-DDC-GCH1 group, and 746.9 ± 129.6% in the LV-TH + DDC-GCH1 group. The relative expression of DDC in the LV-DDC-GCH1 group and the LV-TH + DDC-GCH1 group was 422.4 ± 104.2%, and 309.6 ± 87.7%, respectively.

The concentrations of dopamine secretion in the supernatants of three lentivirus-infectedBMSCs lines were detected by HPLC. The results showed that DA concentrations in the LV-TH group (1 097.00 ± 36.55 ng/mL), the LV-DDC-GCH1 group (709.70 ± 69.83 ng/mL), and the LV-TH + DDC-GCH1 group (4 128.00 ± 92.92 ng/m) were significantly higher than the control group (332.00 ± 10.33 ng/mL) (Fig. 2I). Among them, the content of DA in the LV-TH + DDC-GCH1 group was the highest, which was increased by 12.43-fold compared to the control group. However, DA in cell culture supernatant could be detected by HPLC, but Serotonin (5-hydroxytryptamine, 5-HT) was not detected (Fig. 2J). Therefore, a DA-BMSCs cell line (LV-TH + DDC-GCH1 group) capable of stably and efficiently synthesizing DA neurotransmitters was successfully established.

DA-BMSCs grafts promote behavioral recovery in parkinsonian rats

To evaluate whether genetically engineered BMSCs can be used to rescue PD phenotypes, we transplanted three sets of BMSCs into the MFB of unilateral 6-OHDA-induced PD rats, and a flow chart was indicated in Fig. 3A. A total of approximately 1.0×10^5 cells/graft were stereotactically transplanted into the right MFB of PD model rats at 2 coordinates (Fig. 3B, C). Four weeks after transplantation, the APO-induced rotation behavior of the transplanted rats in the LV-TH group, LV-DDC-GCH1 group, and DA-BMSCs group had a significant reduction compared with the vehicle group (Fig. 3E, H), but the effect of DA-BMSCs group was the most obvious ($P < 0.01$). Furthermore, these improved phenotypes were retained until sacrifice. However, neither PD rats that received BMSCs grafts nor H-DMEM-treated rats showed obvious improvement in APO-induced rotations ($P > 0.05$). Furthermore, the motor coordination ability of the DA-BMSCs group was also effectively improved as assessed by the rotarod test ($P < 0.05$, Fig. 3D, G). Moreover, the rats in the LV-TH group and the DA-BMSCs group were more excited and active than those in the vehicle group 4 weeks and 8 weeks after transplantation, and the total distance of movement was increased significantly in the open-field test ($P < 0.01$; Fig. 3F, I). However, the

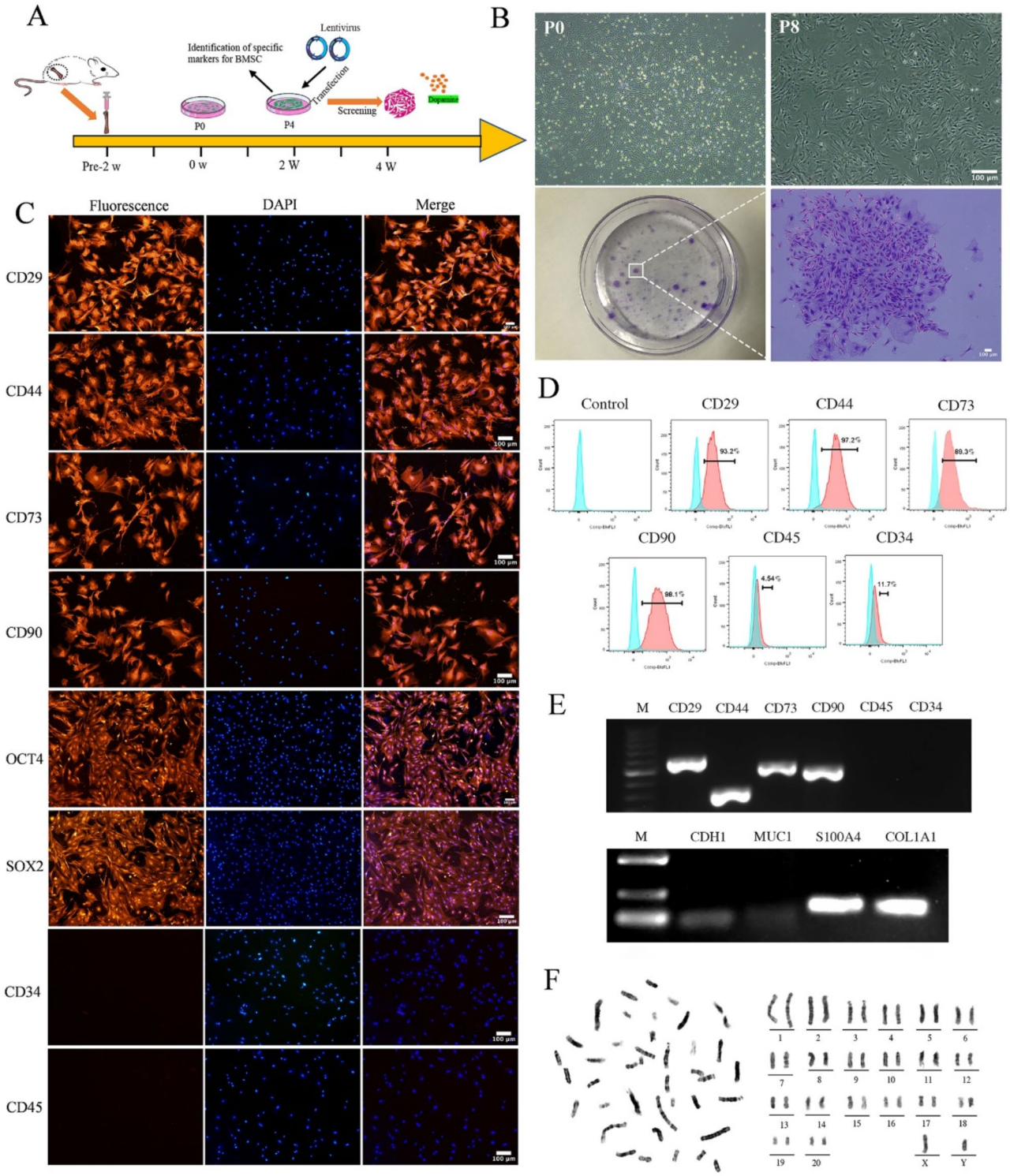

Fig. 1. Cell morphology, colony-forming potentials, specific markers, and karyotypes of rat BMSCs in vitro. (**A**) The timeline for the construction of a cell line of DA-BMSCs capable of stable dopamine production. (**B**) BMSCs morphology and colony forming efficiency of BMSCs at P4 stained with crystal violet. (**C**) Immunofluorescent staining of specific markers of BMSCs. Nearly all the cells expressed MSCs markers CD29, CD44, CD73, CD90, and stem cells markers OCT4, SOX2 (red), and the cell nucleus was shown in blue by DAPI, but did not express CD34 and CD45 (red). (**D**) The expression of specific markers CD29, CD44, CD73, CD90, CD45, and CD34 in BMSCs by Flow cytometry analysis. (**E**) Expression of specific markers genes CD29, CD44, CD73, CD90, CD45, CD34, S100A1 and COL1A1, and epithelial cell markers CDH1, MUC1 were detected by RT-PCR. The original gels are presented in Supplementary Fig. 2 (Fig. S2). (**F**) Chromosome G-banding analysis of rat BMSCs at passage 4. Scale bars represent 100 μm.

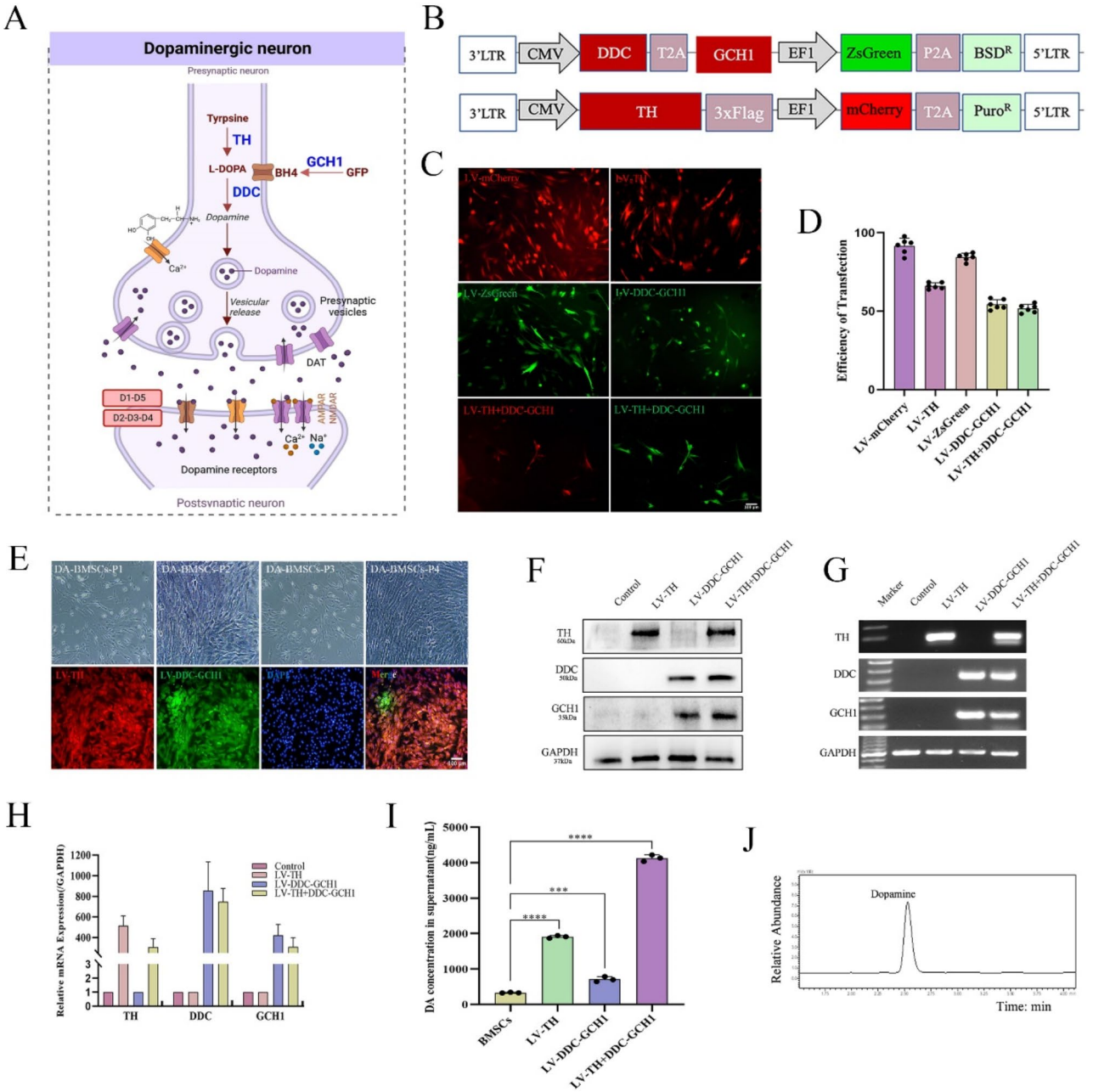

Fig. 2. Construction of lentiviral expression vectors and the establishment of a cell line of DA-BMSCs. (**A**) Dopamine biosynthetic processes involvement in DA-ergic presynaptic and postsynaptic neurons. Dopamine receptor subtypes (D1–D5); DAT dopamine transporter. (**B**) Schematic diagram of lentiviral vectors of LV-TH and LV-DDC-GCH1. (**C**) Fluorescent protein expression of BMSCs 72 h after lentivirus infection of LV-TH and LV-DDC-GCH1. LV-mCherry and LV-ZsGreen represented the control lentivirus. (**D**) The infection efficiency of the above lentivirus ($n = 6$). (**E**) Morphological characteristics of DA-BMSCs (P1–P4) and the expression of fluorescent proteins after puromycin and Blasticidin S selection. (**F**) Western blotting of TH, DDC, and GCH1 proteins in different lentivirus-infected cells. (**G**) RT-PCR analysis of TH, DDC, and GCH1 genes in different lentivirus-infected cells. (**H**) The relative mRNA expression of TH, DDC, and GCH1 was analyzed by RT-qPCR. (**I**) DA concentrations in the cells culture supernatant of each group were detected by HPLC. (**J**) HPLC chromatogram of cells culture supernatant was presented. Scale bars represent 100 μm. All data were presented as mean ± SEM. The *P*-values are from multiple comparisons in one-way ANOVA with Dunnett's multiple comparison test ($n = 3$) $^{***}P < 0.001$, $^{****}P < 0.0001$. The original blots and gels are presented in Supplementary Fig. 2 (Fig. S2).

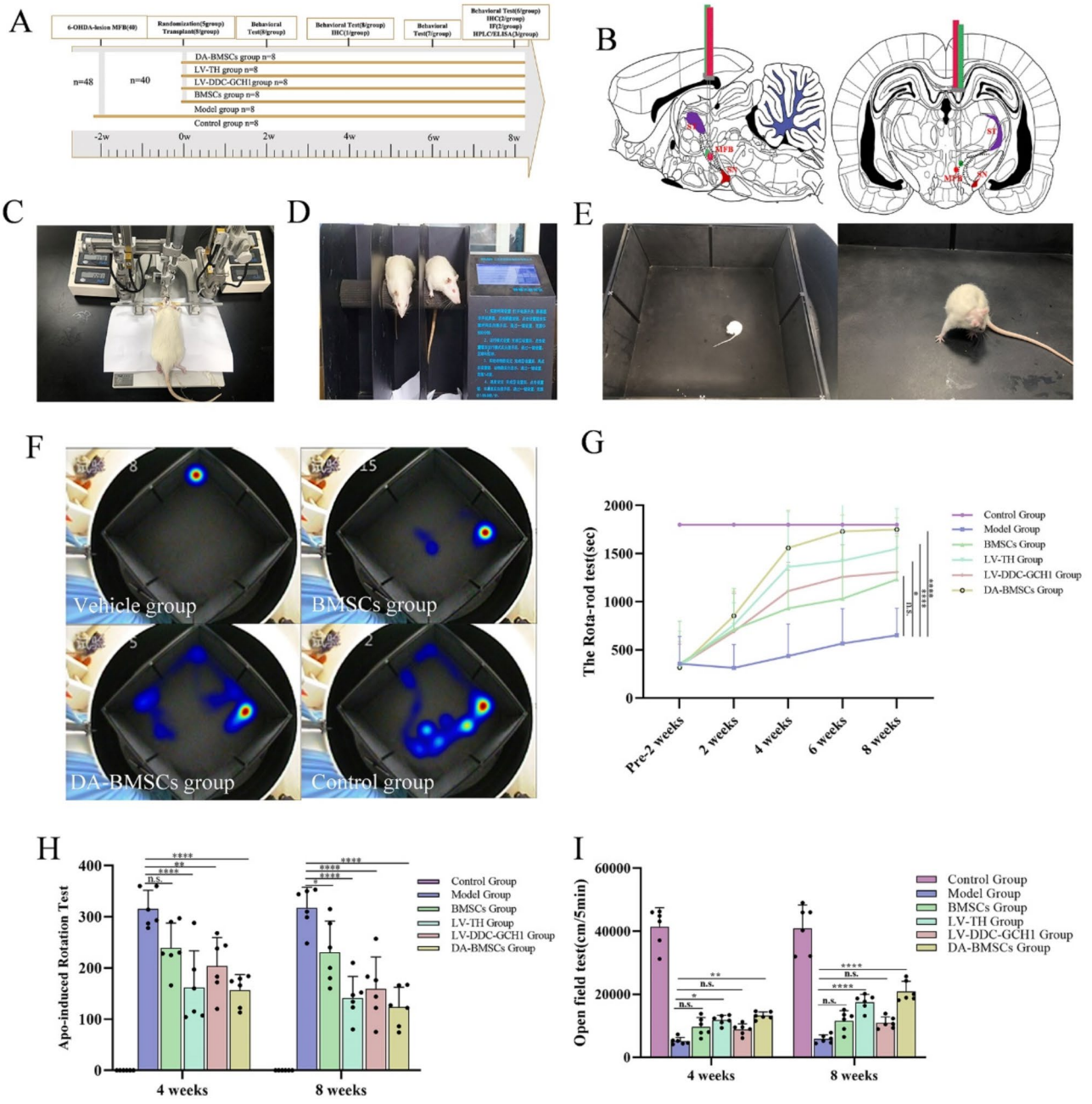

Fig. 3. DA-BMSCs significantly ameliorated the behavioral deficits of a rat model of Parkinson's disease. (**A**) A flow chart depicting the experimental process containing animal groups and the number of animals in each group. (**B**) 6-Hydroxydopamine and DA-BMSCs were stereotactically transplanted into the right medial forebrain bundle (MFB) of each model rat at the two coordinates labeled on the coronal and sagittal planes. (**C**) The PD rats were immobilized on the stereotaxic apparatus, and the cells were injected into the right MFB of the brain. (**D**) Rota-rod test on the Rota-rod apparatus. (**E**) APO-induced rotation test. (**F**) Heat maps of motion trajectory for the open field test. F1: the model group, F2: the BMSCs group, F3: the DA-BMSCs group, and F4: the control group. (**G**) Behavioral evaluation of the rats in the Rota-rod test. (**H**) Behavioral evaluation of the rats in the APO-induced rotation test. (**I**) Behavioral evaluation of the rats in the open field test. All data were presented as mean ± SEM. The *p*-values are from multiple comparisons in two-way ANOVA with Sidak's multiple comparative tests ($n = 6$), $^{*}P < 0.05$, $^{**}P < 0.01$, $^{****}P < 0.0001$, *n.s.* no significance: $P > 0.05$.

movement behavior in the LV-DDC-GCH1 group and the BMSCs group had no significant difference from the vehicle group ($P > 0.05$).

DA-BMSCs differentiated into targeted TH⁺ dopamine neurons in the MFB of PD rat models

Whole-brain hematoxylin and eosin (H&E) analysis revealed the severe loss of neurons in the lesioned area of the PD rat model compared to the healthy side of the brain, and the cells were vacuolated and arranged in disorder (Fig. 4A). Numerous viable transplanted cell grafts were observed and formed an obvious transplanted area in the lesioned brain of PD rats in four BMSCs transplantation groups 8 weeks after transplantation. In addition, the lesioned area was densely surrounded by collagen fibers and inflammatory cells, and fibrotic tissue formed after trauma repair in some areas (Fig. 4A).

TH-3,3′-diaminobenzidine tetrahydrochloride staining of the whole brain showed that, compared to the healthy side, both the TH⁺ cells and the expression level of TH in the lesioned area of PD rats (vehicle group)

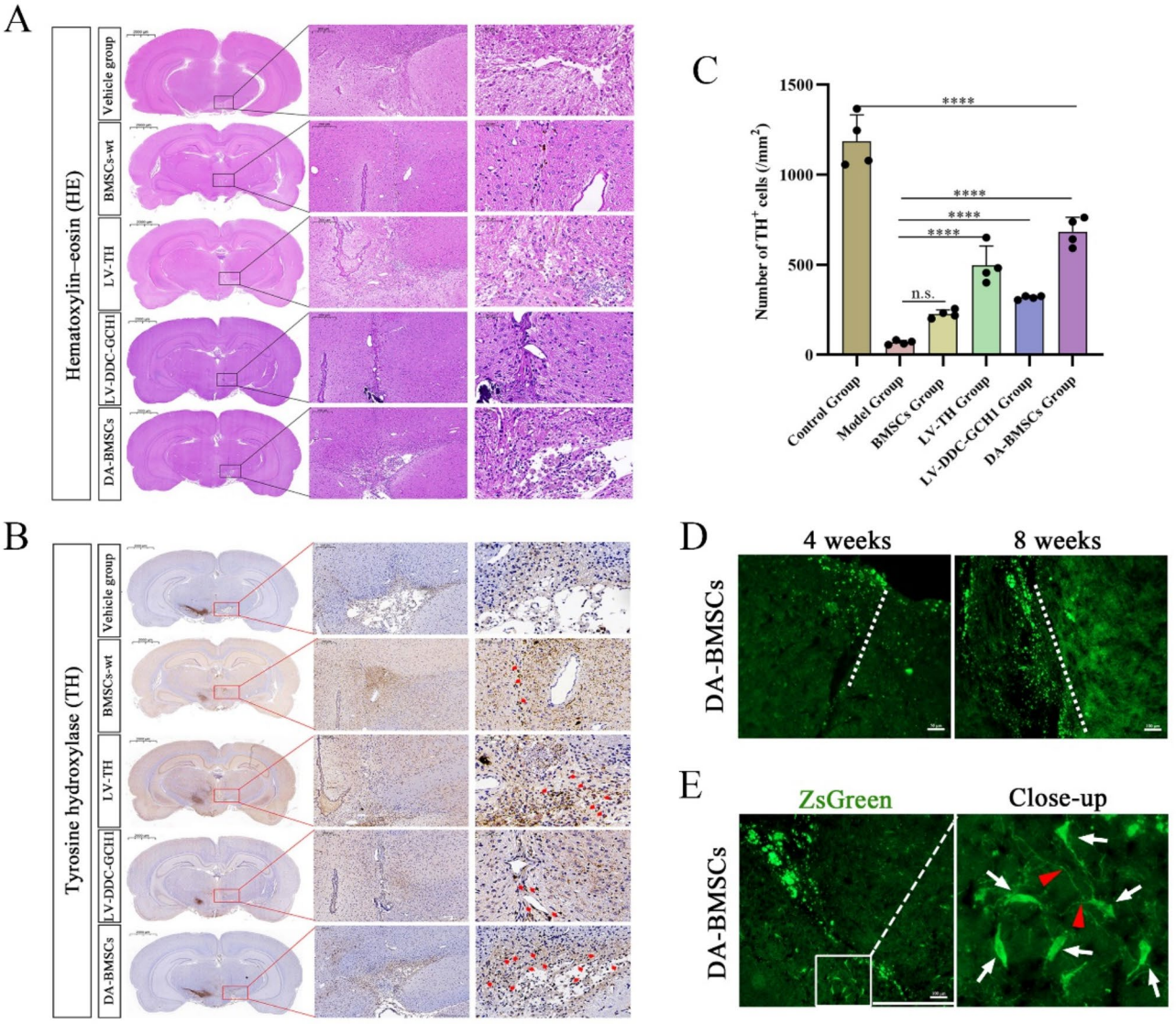

Fig. 4. Effects of DA-BMSCs transplantation on the loss of dopaminergic neurons in the right substantia nigra of PD rat models. (**A**) Representative images of whole-brain with hematoxylin and eosin staining in each group 8 weeks after transplantation. (**B**) Representative images of whole-brain with TH-3,3′-diaminobenzidine staining (TH-DAB) in each group 8 weeks after transplantation. The right image was the higher magnification of the left boxed areas. (**C**) Number of TH⁺ cells in the right substantia nigra of each group. All data were presented as mean ± SEM. The *P*-values are from multiple comparisons in one-way ANOVA with Dunnett's multiple comparison test ($n = 4$), $^{****}P < 0.0001$, *n.s.* no significance: $P > 0.05$. (**D**) DA-BMSCs formed a distinct graft area and migrated from the graft site into the periphery of the injured area, and the migrated distance gradually increased with time. (**E**) The transplanted DA-BMSCs could differentiate into neural cells in the host brain and exhibit neuronal morphology (white arrows) and dendritic structure (red arrow heads) after 8 weeks of transplantation.

were significantly reduced (Fig. 4B). However, numerous TH^+ cells were present in the substantia nigra brain of rats in the LV-TH group and DA-BMSCs group and filled the lesioned area and the periphery area 8 weeks after cell transplantation. The expression of TH was also markedly increased compared with that in the vehicle group under the microscopic image. Moreover, the viable DA neuron number in the MFB of the DA-BMSCs group was significantly higher than that of the vehicle group and other BMSCs transplantation groups according to the result of stereological cell counts of TH^+ dopamine neurons (Fig. 4C). Together, these results revealed that DA-BMSCs significantly increased the number of TH^+ neurons in the lesioned side of the host brain and alleviated motor dysfunction in PD rats. Transplanted DA-BMSCs formed obvious graft areas, and migrated 2.0 mm and 0.5 mm from the graft area into the peripheral brain tissue 8 and 4 weeks after transplantation, respectively (Fig. 4D). Furthermore, DA-BMSCs could differentiate into neural cells in the host brain and exhibit obvious neuronal morphology after 8 weeks of transplantation (Fig. 4E).

DA-BMSCs differentiate into multiple types of functional neurons in the MFB of PD rats

Numerous $mCherry^+/ZsGreen^+$ cells also stained positive for TH, and certain TH^+ cell clusters were scattered throughout the implanted area and integrated into the host brain, which suggested that DA-BMSCs could differentiate into DA neurons in vivo (Fig. 5A). Moreover, the engrafted DA-BMSCs gave rise to various functional neurocytes around and within the graft area 8 weeks after transplantation, which could express the GABAergic neuron marker GABA (Fig. 5B), the glial marker GFAP (Fig. 5C) and the glutamatergic neuronal marker PSD95 (Fig. 5D). These results suggested that the transplanted DA-BMSCs in vivo could survive and differentiate into astrocytes and functional neurons. In addition, the expression of synaptophysin (SYN), a marker of the presynaptic terminal, was significantly increased after DA-BMSCs transplantation. Moreover,

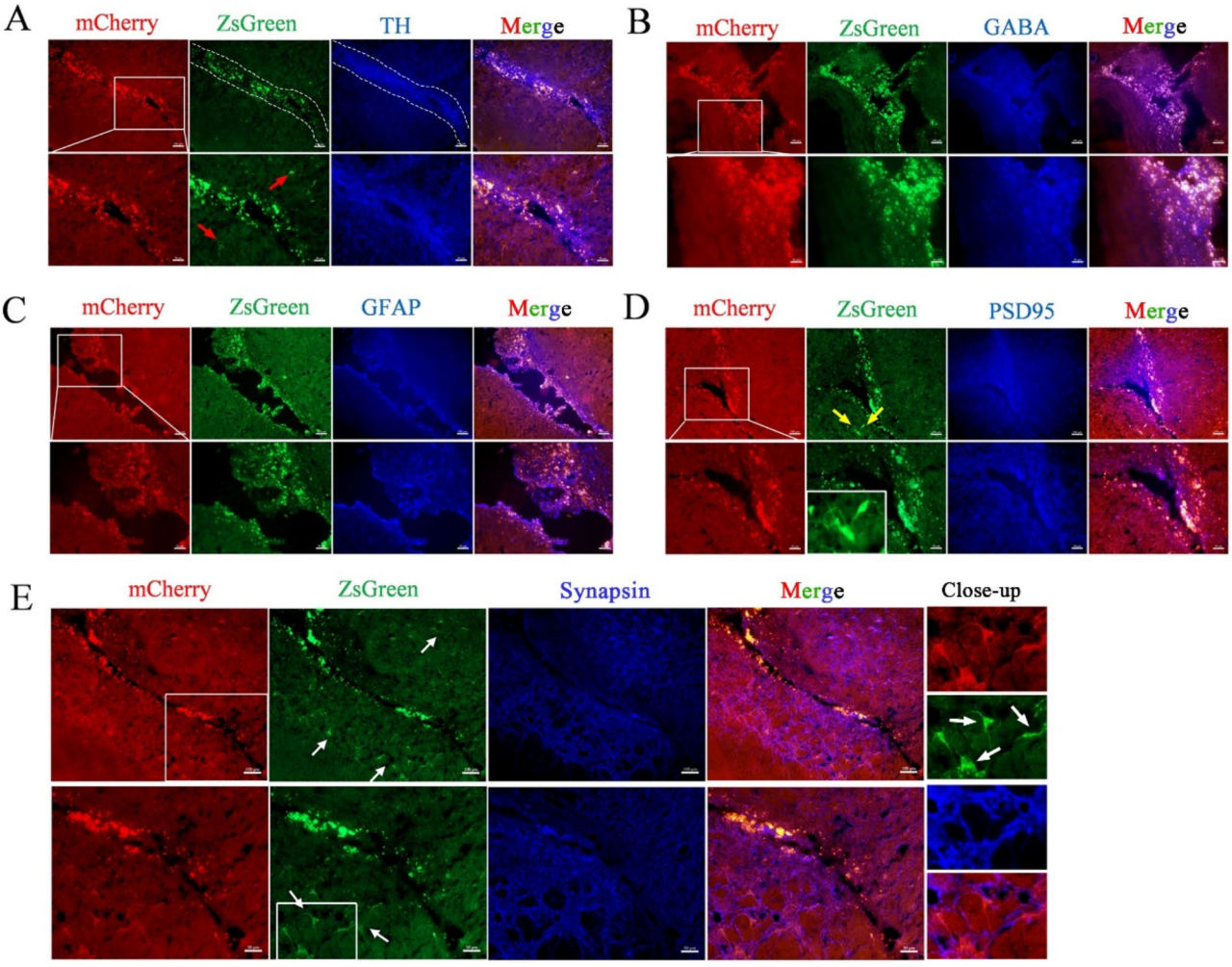

Fig. 5. Survival, differentiation, migration, and integration of transplanted cells in the right hemisphere of PD model rats. (**A–D**) The transplanted DA-BMSCs survived and differentiated into various functional neurons in vivo 8 weeks after transplantation. The TH (**A**), GABA (**B**), GFAP (**C**), and PSD (**D**)-positive cells were detected in the graft region. (**E**) Transplanted DA-BMSCs expressed the marker of mature synapse synaptophysin (SYN) 8 weeks after transplantation. The neuron-like cells derived from the transplanted DA-BMSCs indicated by white arrows formed densely interacting dendritic networks.

numerous SYN$^+$, mCherry$^-$/ZsGreen$^-$ patches were adjacent to the transplanted DA-BMSCs, indicating that host brain-derived neurons connected with DA-BMSCs derived neurons to form mature synapses (Fig. 5E). Importantly, we found that many mCherry$^+$/ZsGreen$^+$ cells assumed neuron-like morphologies with densely interacting dendritic networks (Fig. 5E). The results confirmed that the transplanted DA-BMSCs in the right hemisphere differentiated into functional neurons, migrated into the peripheral damaged areas, integrated with the host brain cells, and participated in the injured tissue repair. Moreover, no evidence of abnormality graft growth was found.

The levels of DA, 5-HT, and inflammatory cytokines in the midbrain and serum

To evaluate the effect of transplanted cells on the post-traumatic inflammatory process of the injured areas, the levels of pro-inflammatory cytokines (IL-6 and TNF-α), and anti-inflammatory cytokines (IL-10) in different groups were detected by ELISA assays 8 weeks after transplantation. As expected, the level of inflammatory cytokines in PD rats after 6-OHDA injection was significantly higher than those in healthy control rats ($P < 0.05$). However, the levels of IL-6, TNF-α, and IL-10 in rats of four BMSC treatment groups were significantly lower than those in the vehicle group ($P < 0.01$) (Fig. 6A). Moreover, the level of inflammatory cytokines in the LV-TH group and DA-BMSCs group decreased most significantly. Interestingly, the most prominent downregulation of inflammatory factors including IL-6, TNF-α, and IL-10, was noted in the LV-TH group at 8 weeks. Moreover, the immunofluorescence results of IBA-1 and C3 in rat brain sections showed that, compared with the model group, the expression levels of IBA-1 and C3 were significantly reduced in the DA-BMSCs group (Fig. 6B). The results confirmed that genetically engineered BMSCs retained the ability to repair and exerted superior efficacy on the post-traumatic inflammatory process.

To evaluate whether the improvement in the phenotype of PD rats grafted with DA-BMSCs is attributed to the secretion of dopamine transmitters, we analyzed the DA and 5-HT levels in cerebrospinal fluid and serum 8 weeks after transplantation by HPLC. As anticipated, the DA-BMSCs group showed the most obvious upregulation of DA level in CSF and serum (21.531 ± 1.031 ng/mg and 6.547 ± 0.036 ng/mL, respectively) (Fig. 6C, E), as well as 5-HT (0.433 ± 0.035 ng/mg and 0.971 ± 0.043 ng/mL) (Fig. 6D and E), compared to the vehicle group (DA: 9.249 ± 0.449 ng/mg and 4.180 ± 0.069 ng/mL, 5-HT:0.173 ± 0.007 ng/mg and 0.085 ± 0.005 ng/mL). Furthermore, the dopamine receptor expression was evaluated with immunofluorescence staining. The results showed that the DA-BMSCs group exhibited significant upregulation of dopamine receptor DRD1 expression compared to the model group (Fig. 6F). The significant restoration of DA and 5-HT in the presence of DA-BMSCs reflected the restoration of the DA biosynthesis pathway and function in vivo. Together, these results indicated that grafts of DA-BMSCs alleviated motor dysfunction in PD rats through the secretion of dopamine transmitters.

Discussion

The main pathological feature of PD is the massive death of dopaminergic neurons in the ventral midbrain, resulting in decreased synthesis of dopamine (DA) in the striatum[10,35]. Strategies have been aimed at increasing dopamine levels, improving neuronal survival, and replacing lost dopamine neurons using stem cell transplantation[36]. One of the important options for the treatment of PD is to upregulate the DA levels in the striatum by increasing the levels of DA synthase enzymes. TH, DDC, and GCH1 are three key enzymes in the dopamine synthesis pathway[37]. Previous studies have shown that adenoviral vectors AAV-TH, AAV-DDC, and AAV-GCH1, which were injected into the striatum of PD animal models, could upregulation the DA level in the brain and had significant effects on the dyskinesias[37]. Gene therapy has been an attractive approach to reestablishing dopamine levels and restoring the nigrostriatal pathway to improve dopaminergic network function through the introduction of enzymatic enhancement of dopamine production by virus delivery[10]. Furthermore, a clinical trial demonstrated that vectors carrying TH, DDC, and GCH1 were safe for PD patients and improved the motor effect[10]. Compared with adenoviral vectors, lentiviral vectors have a series of advantages such as continuous expression of target genes and large packaging capacity (8–9 kb)[38]. However, the difficulties in precisely controlling the expression level of exogenous genes, the potential oncogenicity of viral genes, or other unexpected consequences of insertional mutagenesis severely limited its widespread clinical application.

Considering the safety and efficacy issues of viral vector-mediated gene therapy for Parkinson's disease, such as the lack of selectivity of virus-infected cells and interference with normal cell function, we developed a new strategy to treat PD by delivering dopamine to the striatum continuously through genetically engineered BMSCs stably expressing DA (DA-BMSCs) with lentivirus-mediated genes and explored the survival and plasticity of DA-BMSCs in the brains of PD rats. In this study, Due to the excessive length (> 10 kb) of the total sequence of TH, DDC, and GCH1, we constructed two lentiviral vectors, one carrying the TH gene and mCherry fluorescent reporter gene, and the other carrying the DDC and GCH1 sequence and ZsGreen fluorescent reporter gene.

Over the past few decades, many cell types have been identified as candidates to replace dying dopaminergic neurons, including cells derived from the fetal ventral midbrain, neural stem cells, mesenchymal stem cells, and dopaminergic progenitors/neurons differentiated from pluripotent stem cells[39]. However, limitations remain, including low survival rates of transplanted cells and a requirement to differentiate into mature dopamine neurons and establish a functional circuit with host neurons before functioning in vivo. As predicted, the PD rats of the BMSCs group showed certain motor functional improvements until 8 weeks after transplantation. In this study, we used a new strategy to quickly restore local dopamine levels in the midbrain of PD rats by DA-BMSC transplantation. These PD model rats of the DA-BMSCs group exhibited significant behavioral improvements within 4 weeks of transplantation, which revealed that DA-BMSCs had more distinct advantages in improving motor disorders of PD. Importantly, most Parkinson's disease rats (7/8) exhibited long-term benefits through only one DA-BMSCs transplant.

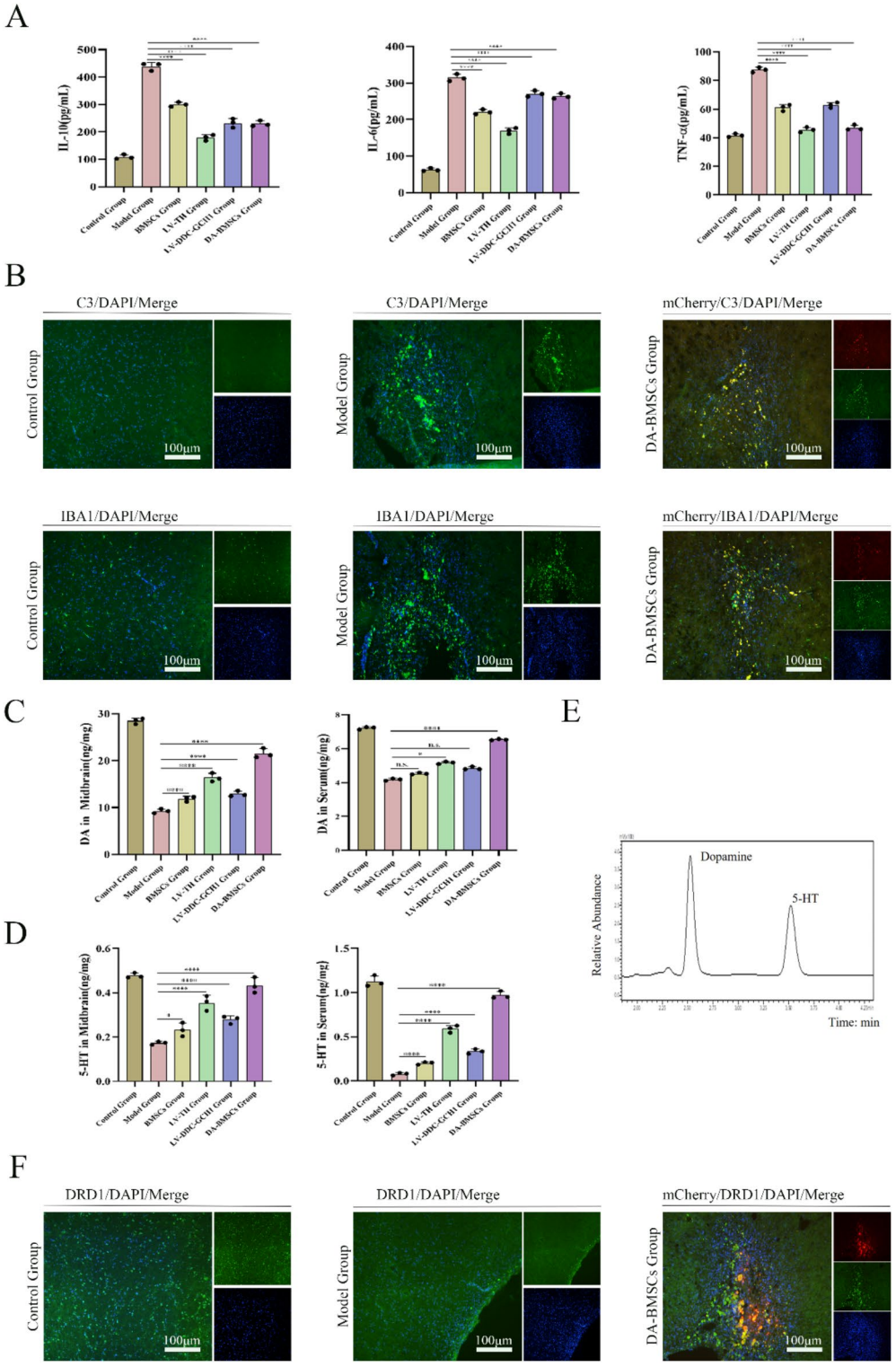

Fig. 6. The levels of IL-6, TNF-α and IL-10 in the midbrain, and the levels of DA and 5-HT in the midbrain and serum, and the expression levels of IBA-1, C3 and DRD1 in the midbrain. (**A**) The expression of inflammatory factors including IL-6, TNF-α, and IL-10, were effectively inhibited in the absence or presence lentivirus-infected of BMSCs, which played an important role in the process of injury repair. (**B**) The expression levels of IBA-1 and C3 were significantly reduced in the DA-BMSCs group compared to the model group. (**C**, **D**) A significant reduction of DA and 5-HT levels in the midbrain of the injured side and the serum was confirmed, and the effect could be significantly restored to normal levels by DA-BMSCs. (**E**) An HPLC chromatogram of serum was presented. (**F**) The DA-BMSCs group exhibited significant upregulation of DRD1 expression compared to the model group. All data were presented as mean ± SEM. The *P*-values are from multiple comparisons in one-way ANOVA with Dunnett's multiple comparison test ($n = 3$), $^{*}P < 0.05$, $^{****}P < 0.0001$, *n.s.* no significance: $P > 0.05$.

Furthermore, our research demonstrated that DA-BMSCs transplanted into the right hemisphere of PD rats could survive for the long term and significantly increased the number of dopaminergic neurons in the substantia nigra. Moreover, the number of functional neurons and astrocytes differentiated from DA-BMSCs in injured areas significantly increased, migrated to the graft periphery, and tightly connected with the host brain tissue. Many surviving DA neurons derived from DA-BMSCs were indicated to serve an important role in the behavioral recovery of motor dysfunction. GABAergic neurons derived from the DA-BMSCs may be responsible for regulating the balance of excitatory and inhibitory signals in the dopamine pathway. In addition, the formation of mature synapse formation between donor and host-derived neurons could also promote functional recovery and neurological function in rats with PD.

Proinflammatory mediators released in the process, including matrix metalloproteinases, tumor necrosis factor-alpha (TNF-α), interleukin (IL)-6, IL-10, and cytokine-induced neutrophil chemoattractant (CINC-1), have been shown to contribute to the development of brain injury[40]. In the present study, the secretion of inflammatory factors IL-6, TNF-α, and IL-10 were significantly inhibited 4 weeks of transplantation of DA-BMSCs, resulting in neuroprotective effects, which was consistent with previous studies[41,42]. The cytokines are released from several cell types and can be synthesized in the central nervous system (CNS) by microglia, astrocytes, and some populations of neurons. The MSCs in the host brain could promote the switch of microglia from M1 phenotype-producing inflammatory factors to M2 phenotype-protecting neurons, thereby having important effects on anti-inflammatory and neuron survival[43]. The present study demonstrated that the expression levels of IBA-1 and C3 were significantly reduced in the DA-BMSCs group compared to the model group. This finding suggested that DA-BMSCs may exert a modulatory effect on the activation of microglia and the complement system, which are key players in neuroinflammatory responses. This modulation of IBA-1 and C3 expression by DA-BMSCs might interact with microglial cells or astrocytes to modulate their phenotype and reduce the release of inflammatory molecules. Further studies are needed to elucidate the precise mechanisms underlying these effects.

Serotonin (5-HT) is an inhibitory neurotransmitter that plays an important role in the regulation of mood and social behavior, and its dysfunction is closely associated with the onset or progression of Parkinson's disease[44]. The levels of DA and 5-HT in cerebrospinal fluid and serum of PD rats receiving DA-BMSCs graft were significantly up-regulated. In addition, the treatment effect of the LV-TH group was significantly more prominent than that of the LV-DDC-GCH1 group, which also confirmed the results of the previous study. Although the DA level of the DA-BMSCs group was significantly upregulated compared with the vehicle group, it did not reach the normal level of DA 8 weeks after transplantation. It may be due to the uncontrollable differentiation direction of transplanted DA-BMSCs in vivo, and some graft-derived cells may inhibit the upregulation of DA levels. On the other hand, overexpressed TH, DDC, and GCH1 might be feedback-inhibited, resulting in decreased DA expression. Furthermore, the dopamine receptor DRD1 expression in DA-BMSCs group significantly upregulated compared to the model group. These findings suggest that the increased dopamine secretion in DA-BMSCs has a significant physiological impact on the cells, potentially modulating their behavior and therapeutic efficacy and support the potential use of DA-BMSCs in the treatment of Parkinson's disease.

In summary, we successfully established a genetically engineered mesenchymal stem cell line encoding three critical genes for dopamine synthesis (DA-BMSCs). Furthermore, the transplanted DA-BMSCs could survive in PD rats' brain microenvironment for at least 8 weeks and differentiated into various functional neurocytes to significantly improve motor and nonmotor function in the rat model of PD over a relatively long period. Thus, our results will contribute to the development of genetically engineered stem cells that serve as attractive donor materials for neuroscience research and the treatment of neurodegenerative diseases.

Data availability

The datasets used and/or analyzed during the current study are available from the corresponding author upon reasonable request.

Received: 30 August 2024; Accepted: 6 April 2025
Published online: 11 April 2025

References

1. Ivanidze, J. et al. Molecular imaging of striatal dopaminergic neuronal loss and the neurovascular unit in Parkinson disease. *Front. Neurosci.-Switz.* **14**, 1 (2020).
2. Kikuoka, R. et al. Mirtazapine exerts astrocyte-mediated dopaminergic neuroprotection. *Sci. Rep. U.K.* **10**, 1 (2020).
3. Li, B. et al. Acetylation of NDUFV1 induced by a newly synthesized HDAC6 inhibitor HGC rescues dopaminergic neuron loss in Parkinson models. *Iscience* **24**, 1 (2021).
4. Armstrong, M. J. & Okun, M. S. Diagnosis and treatment of Parkinson disease: A review. *J. Am. Med. Assoc.* **323**, 548 (2020).
5. Zheng, C. Q. et al. Resveratrol alleviates levodopa-induced dyskinesia in rats. *Front. Immunol.* **12**, 1 (2021).
6. Wu, C. Q. et al. The effect of dopamine replacement therapy on cortical structure in Parkinson's disease. *Cns Neurosci. Ther.* **1**, 1 (2023).
7. Guo, Y. et al. Neural progenitor cells derived from fibroblasts induced by small molecule compounds under hypoxia for treatment of Parkinson's disease in rats. *Neural Regen. Res.* **18**, 1090–1098 (2023).
8. Zhang, L., Lin, Y. X., Bai, W. S., Sun, L. & Tian, M. Human umbilical cord mesenchymal stem cell-derived exosome suppresses programmed cell death in traumatic brain injury via PINK1/Parkin-mediated mitophagy. *Cns Neurosci. Ther.* **29**, 2236–2258 (2023).
9. Guo, Y. et al. Miniature-swine iPSC-derived GABA progenitor cells function in a rat Parkinson's disease model. *Cell Tissue Res.* **1**, 1 (2023).
10. Li, J. et al. Genetically engineered mesenchymal stem cells with dopamine synthesis for Parkinson's disease in animal models. *Npj Parkinsons Dis.* **8**, 1 (2022).

11. Chen, Y. et al. Clinical and genetic heterogeneity in a cohort of Chinese children with dopa-responsive dystonia. *Front. Pediatr.* **8**, 1 (2020).
12. Falcon, T. et al. Exploring integument transcriptomes, cuticle ultrastructure, and cuticular hydrocarbons profiles in eusocial and solitary bee species displaying heterochronic adult cuticle maturation. *PLoS ONE* **14**, 1 (2019).
13. Dai, D. F. et al. Peli1 controls the survival of dopaminergic neurons through modulating microglia-mediated neuroinflammation. *Sci. Rep. U.K.* **9**, 1 (2019).
14. Shen, Y. et al. Triple transduction with adeno-associated virus vectors expressing tyrosine hydroxylase, aromatic-L-amino-acid decarboxylase, and GTP cyclohydrolase I for gene therapy of Parkinson's disease. *Hum. Gene Ther.* **11**, 1509 (2000).
15. Lu-Nguyen, N. B. et al. Transgenic expression of human glial cell line-derived neurotrophic factor from integration-deficient lentiviral vectors is neuroprotective in a rodent model of Parkinson's disease. *Hum. Gene Ther.* **25**, 631 (2014).
16. Torres, E. M., Monville, C., Lowenstein, P. R., Castro, M. G. & Dunnett, S. B. Delivery of Sonic Hedgehog or glial derived neurotrophic factor to dopamine-rich grafts in a rat model of Parkinson's disease using adenoviral vectors increased yield of dopamine cells is dependent on embryonic donor age. *Brain Res. Bull.* **68**, 31–41 (2005).
17. Cederfjll, S., Bjrklund & Kirik & Design of a single AAV vector for coexpression of TH and GCH1 to Establish continuous DOPA synthesis in a rat model of Parkinson's disease. *Mol. Ther.* **20**, 1315–1326 (2012).
18. Badin, R. A. et al. Gene therapy for Parkinson's disease: preclinical evaluation of optimally configured TH:CH1 fusion for maximal dopamine synthesis. *Mol. Ther. Method Clin. D* **14**, 206–216 (2019).
19. Li, H. & Yue, B. Effects of various antimicrobial agents on multi-directional differentiation potential of bone marrow-derived mesenchymal stem cells. *World J. Stem Cells* **11**, 322–336 (2019).
20. Terashima, T. et al. Enhancing the therapeutic efficacy of bone marrow-derived mononuclear cells with growth factor-expressing mesenchymal stem cells for ALS in mice. *Iscience* **23**, 1 (2020).
21. Alexander, T. & Greco, R. Hematopoietic stem cell transplantation and cellular therapies for autoimmune diseases: overview and future considerations from the autoimmune diseases working party (ADWP) of the European society for blood and marrow transplantation (EBMT). *Bone Marrow Transpl.* **57**, 1055–1062 (2022).
22. Harrell, C. R., Jovicic, N., Djonov, V., Arsenijevic, N. & Volarevic, V. Mesenchymal stem cell-derived exosomes and other extracellular vesicles as new remedies in the therapy of inflammatory diseases. *Cells* **8**, 1 (2019).
23. Chen, Y., Shen, J. B., Ke, K. F. & Gu, X. S. Clinical potential and current progress of mesenchymal stem cells for Parkinson's disease: a systematic review. *Neurol. Sci.* **41**, 1051–1061 (2020).
24. Puranik, N., Arukha, A. P., Yadav, S. K., Yadav, D. & Jin, J. O. Exploring the role of stem cell therapy in treating neurodegenerative diseases: challenges and current perspectives. *Curr. Stem Cell Res. Therapy* **17**, 113–125 (2022).
25. Geng, X. et al. BDNF alleviates Parkinson's disease by promoting STAT3 phosphorylation and regulating neuronal autophagy. *Cell Tissue Res.* **393**, 455–470 (2023).
26. Zeng, X. S., Geng, W. S., Jia, J. J. & Wang, Z. Q. Advances in stem cells transplantation for the therapy of Parkinson's disease. *Curr. Stem Cell Res. Therapy* **16**, 958–969 (2021).
27. Sert, N. P. D., Hurst, V., Ahluwalia, A., Alam, S. & Würbel, H. The ARRIVE guidelines 2.0: updated guidelines for reporting animal research. *BMC Vet. Res.* **16**, 242 (2020).
28. Xu, J. J. et al. Therapeutic function of a novel rat induced pluripotent stem cell line in a 6-OHDA-induced rat model of Parkinson's disease. *Int. J. Mol. Med.* **50**, 1 (2022).
29. Guo, Y. et al. Multiple functions of reversine on the biological characteristics of sheep fibroblasts. *Sci. Rep. U.K.* **11**, 1 (2021).
30. Bárbara, M. P. et al. Secretome of undifferentiated neural progenitor cells induces histological and motor improvements in a rat model of Parkinson's disease. *Stem Cells Transl. Med.* **11**, 1 (2018).
31. Sun, Y. et al. Engrafted primary type-2 astrocytes improve the recovery of the nigrostriatal pathway in a rat model of Parkinson's disease. *Mol. Cell. Biochem.* **476**, 619–631 (2021).
32. Woo, J. et al. Control of motor coordination by astrocytic tonic GABA release through modulation of excitation/inhibition balance in cerebellum. *Proc. Natl. Acad. Sci. U.S.A.* **115**, E5253 (2018).
33. Pinheiro, B., Anjo, S. I., Manadas, B., Silva, J. D. D. & Salgado, A. J. Bone marrow mesenchymal stem cells' secretome exerts neuroprotective effects in a Parkinson's disease rat model. *SSRN Electron. J.* **1**, 1 (2019).
34. Farhadi, M. et al. Implantation of human olfactory ecto-mesenchymal stem cells restores locomotion in a rat model of Parkinson's disease. *J. Chem. Neuroanat.* **114**, 101961 (2021).
35. Xiao, Z. Z. et al. The potential therapy with dental tissue-derived mesenchymal stem cells in Parkinson's disease. *Stem Cell Res. Ther.* **12**, 1 (2021).
36. Hiller, B. M. et al. Optimizing maturity and dose of iPSC-derived dopamine progenitor cell therapy for Parkinson's disease. *Npj Regen. Med.* **7**, 1 (2022).
37. Koo, T., Popplewell, L., Athanasopoulos, T. & Dickson, G. Triple trans-splicing adeno-associated virus vectors capable of transferring the coding sequence for full-length dystrophin protein into dystrophic mice. *Hum. Gene Ther.* **25**, 98–108 (2014).
38. Zheng, C. X. et al. Lentiviral vectors and adeno-associated virus vectors: useful tools for gene transfer in pain research. *Anat. Rec.* **301**, 825–836 (2018).
39. Parmar, M., Grealish, S. & Henchcliffe, C. The future of stem cell therapies for Parkinson disease. *Nat. Rev. Neurosci.* **21**, 103–115 (2020).
40. Barichello, T. et al. TNF-alpha, IL-1beta, IL-6, and cinc-1 levels in rat brain after meningitis induced by *Streptococcus pneumoniae*. *J. Neuroimmunol.* **221**, 42–45 (2010).
41. Li, A. et al. Delivery of exogenous proteins by mesenchymal stem cells attenuates early memory deficits in a murine model of Alzheimer's disease. *Neurobiol. Aging* **86**, 81–91 (2020).
42. Zhou, L. P. et al. Neuroprotective effects of human umbilical cord mesenchymal stromal cells in PD mice via centrally and peripherally suppressing NLRP3 inflammasome-mediated inflammatory responses. *Biomed. Pharmacother.* **153**, 1 (2022).
43. Asveda, T., Talwar, P. & Ravanan, P. Exploring microglia and their phenomenal concatenation of stress responses in neurodegenerative disorders. *Life Sci.* **328**, 1 (2023).
44. Charnay, Y. & Léger, L. Brain serotonergic circuitries. *Dialog. Clin. Neurosci.* **12**, 471–487 (2010).

Author contributions

Y.G. and C.L concepted and designed the experiments; J.C., P.Y., and Y.H. established the Parkinson's disease models and analyzed data; C.W. and Y.L. performed other experiments and collected data; J.F. and W.D. analyzed statistical; C.M. and G.L. wrote manuscript draft. All authors revised the manuscript and approved the final manuscript.

Funding

This research was supported by the National Natural Science Foundation of China (NSFC Grant Nos. 82371382, 81771381), the Natural Science Foundation of the Higher Education Institutions of Anhui Province (Grant Nos. KJ2021ZD0085, 2022AH051434, 2024AH040193, and 2024AH051296), the Anhui Provincial Key Research and

Development Project (Grant Nos. 2022e07020030 and 2022e07020032), the Science Research Project of Bengbu Medical College (Grant Nos. 2021byfy002), the Postgraduate Innovative Training Program of Bengbu Medical College (Grant Nos. Byycx21050, Byycx23006) and the Undergraduate Innovative Training Program of China (Grant Nos. 202310367015, 202410367002, 202410367012, 202410367079).

Declarations

Competing interests
The authors declare no competing interests.

Ethical approval
All animal experiments were performed in line with the principles of the Chinese Laboratory Animal Management and were approved by the Ethics Committee of Bengbu Medical College (Bengbu, China; approval no. 2022-139). The present study is reported in accordance with ARRIVE guidelines.

Additional information
Supplementary Information The online version contains supplementary material available at https://doi.org/10.1038/s41598-025-97557-4.

Correspondence and requests for materials should be addressed to Y.G. or C.L.